A Time-Efficient Fractional Vegetation Cover Estimation Method Using the Dynamic Vegetation Growth Information From Time Series GLASS FVC Product

Yixuan Tu, Kun Jia, Xiangqin Wei, Yunjun Yao, Mu Xia, Xiaotong Zhang, and Bo Jiang

***Abstract*— Fractional vegetation cover (FVC) is an important land surface parameter for many environmental and climate-related modeling and agricultural applications. Incorporating vegetation growth information into FVC estimation process could effectively improve FVC estimation accuracy. Methods utilizing vegetation growth information from field measurement and coarse resolution FVC product have been developed recently to estimate site-scale and finer spatial resolution FVC, and achieved satisfactory performances. However, the computational efficiency of these methods is not satisfactory and they are only feasible for analyzing historical data containing a complete vegetation growth cycle. This letter developed a time-efficient FVC estimation method at Landsat scale based on temporally rich data from coarse spatial resolution Global LAnd Surface Satellite (GLASS) FVC, which facilitates development of a time-efficient dynamic vegetation growth model, and radiative transfer models linking Landsat 7 reflectance to FVC, and all combined in a probabilistic dynamic Bayesian network (DBN) framework. In addition, the proposed method is also suitable for real-time FVC estimation and has the potential to be applied on a larger scale. Validation results indicate that the performance of the proposed method is satisfactory ($R^2 = 0.889$, RMSE $= 0.0917$) and comparable to previously developed inefficient but well-established FVC estimation method incorporating the vegetation growth model represented by modified Verhulst logistic equation ($R^2 = 0.884$, RMSE $= 0.0913$).**

***Index Terms*— Dynamic vegetation characteristics, fractional vegetation cover (FVC), Global LAnd Surface Satellite (GLASS) FVC product.**

I. Introduction

FRACTIONAL vegetation cover (FVC) is defined as the fraction of green vegetation of the total statistical area in the nadir view [1], [2]. It is an important parameter for studying atmosphere, pedosphere, hydrosphere, biosphere and their interactions in the earth system [3], [4]. Remote sensing technology provides an effective means to estimate FVC at regional and global scales [5]. FVC generated from remotely sensed data could be used to characterize vegetation changes caused by environmental factors and climatic conditions over large regions. However, the accuracy of current FVC estimation methods for a single remote sensing image is possibly influenced by cloud and aerosol contamination.

Vegetation growth characteristics are often described by features or indices of aboveground vegetation parts, such as vegetation cover, plant height, biomass and species abundance distribution. The vegetation growth information is important for depicting the vegetation growth process and contains particular information for FVC estimation. Dynamic vegetation growth models which represent vegetation growth characteristics have been developed in many studies, including many mechanical or semimechanical dynamic vegetation growth models [6]. Furthermore, FVC estimating methods incorporating dynamic vegetation growth models have been developed recently to make the models more robust against the influence of atmospheric condition on remote sensing data and improve FVC estimation accuracy. Initially, the FVC estimation method for MODIS pixels incorporating dynamic vegetation growth model built using field FVC measurements and radiative transfer model was developed, and significantly improved FVC estimation accuracy compared to the commonly used lookup table (LUT) method [7]. However, collecting sufficient field measurements to build dynamic vegetation growth models for each pixel of remote sensing data on a large scale was impossible. To solve the problem of limited field data, the method was improved to estimate finer resolution FVC in which several finer resolution pixels sharing the same dynamic vegetation growth model built on the corresponding time series coarse resolution FVC product in a homogeneous area [8]. Besides, the method was further improved for FVC estimation in heterogeneous areas, which employed a decomposing approach to build independent dynamic vegetation growth model for each finer resolution pixel [9].

These methods took advantage of vegetation growth characteristics on FVC estimation process, and the FVC estimation errors caused by cloud contamination were reduced, and significantly improved the finer resolution FVC estimation accuracy. However, the computational costs of these methods are too high because of the time-consuming iteration process for fitting dynamic vegetation growth models using the Verhulst logistic equation. In addition, these methods are only feasible when the observations (remotely sensed data and coarse resolution FVC product) of the whole vegetation growth

Manuscript received January 23, 2019; revised July 3, 2019 and September 24, 2019; accepted November 4, 2019. Date of publication December 3, 2019; date of current version September 25, 2020. This work was supported in part by the National Natural Science Foundation of China under Grant 41671332 and Grant 41571422, in part by the National Key Research and Development Program of China under Grant 2016YFA0600103, and in part by the Tang Scholar Program. The work of K. Jia was supported by the Tang Scholar of Beijing Normal University. *(Corresponding author: Kun Jia.)*

Y. Tu, K. Jia, Y. Yao, M. Xia, X. Zhang, and B. Jiang are with the State Key Laboratory of Remote Sensing Science, Beijing Engineering Research Center for Global Land Remote Sensing Products, Faculty of Geographical Science, Beijing Normal University, Beijing 100875, China (e-mail: jiakun@bnu.edu.cn).

X. Wei is with the Institute of Remote Sensing and Digital Earth, Chinese Academy of Sciences, Beijing 100101, China (e-mail: weixq@radi.ac.cn).

Color versions of one or more of the figures in this letter are available online at http://ieeexplore.ieee.org.

Digital Object Identifier 10.1109/LGRS.2019.2954291

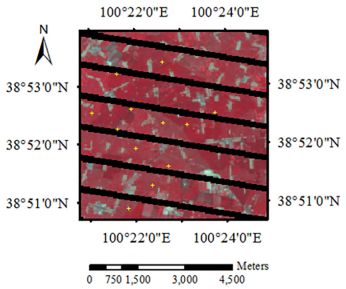

Fig. 1. Geographic location of the study area. The yellow-cross markers on the false color composite imagery show the location of the field survey sites.

cycle are available beforehand to build the dynamic vegetation growth model. Real-time and rapid FVC estimation on a large scale could not be accomplished using these methods. Therefore, there is an urgent need to develop a time-efficient finer resolution FVC estimation method employing dynamic vegetation growth information to achieve high-quality FVC estimates on large scale.

This letter aims to propose a time-efficient finer resolution FVC estimating method incorporating dynamic vegetation growth information from time series coarse resolution FVC product. The method should be able to estimate real-time FVC when remote sensing observations are updated. In addition, the building of dynamic vegetation growth models should have fast calculating speed by reducing iteration times. In this letter, dynamic vegetation growth models were built for each Landsat 7 ETM+ pixel using time series of the Global Land Surface Satellite (GLASS) FVC product. Then, a radiative transfer model was used to establish a relationship between spectral reflectance and FVC. Next, the above two components were combined in a dynamic Bayesian network (DBN) probabilistic framework to achieve the optimal FVC estimation at the finer-scale Landsat resolution. Finally, validation of the proposed method was conducted by the direct comparison between the estimated FVC and the field measured FVC.

II. Study Area and Data

A. Study Area

The study area is in part of the Yingke oasis region, which is located in the Heihe River Basin in Northwest China. This area belongs to an arid region where annual average precipitation and temperature is 140 mm and 7–10 °C, respectively. The main land cover type of the study area is farmland planted with maize. The geographic location of the selected study area is shown in Fig. 1 based on a Landsat 7 ETM+ image acquired on June 24. Thirteen sample sites were selected and the size of each one was 10 m × 10 m. These sites are covered with maize. Ground surveys covering the whole growing season of maize were conducted from May 24, 2012 to August 28, 2012. Nine photographs were taken at each sampling site, with one at the center and the others along with the two diagonals of each site. The FVC of the sample sites was calculated by averaging FVC values from the nine digital photographs. The FVC values from the photographs were determined using an automatic shadow-resistant segmentation algorithm, which could achieve similar performance as visual interpretation [10].

B. GLASS FVC Product

The GLASS FVC product, generated from eight days MODIS reflectance data (MOD09A1) at a spatial resolution of 500 m using machine learning methods, was adopted as the time series coarse-resolution FVC product in this letter [11], [12]. To keep consistency with Landsat 7 ETM+ reflectance data, GLASS FVC data were reprojected to the Universal Transverse Mercator (UTM) projection using the MODIS Reprojection Tools (MRT). Then, the time series GLASS FVC data were filtered using Savitzky–Golay algorithm [13] to reduce the noise disturbance. There are two parameters to set in Savitzky–Golay algorithm, the half-width of the smoothing window (m) and the degree of the smoothing polynomial (d). The combination of (m, d) was set to (4, 6), which was proven to provide the best-fitting effect in most cases.

C. Landsat 7 ETM+ Reflectance Data

The Landsat 7 ETM+ reflectance data (Path 133, Row 033) corresponding to the field survey data were obtained from the U.S. Geological Survey's (USGS) earth explorer. Eight images from day of year (DOY) 160–272 in the year 2012, covering the whole growth period of maize, were used in this letter. The Landsat Ecosystem Disturbance Adaptive Processing System software was used to conduct the radiometric calibration and atmospheric correction of these data. Since the failure of scan line corrector (SLC) causing off data gaps, the Geostatistical Neighborhood Similar Pixel Interpolator (GNSPI) algorithm was applied to fill the gaps of the data with predicted reflectance values [14].

III. Methods

Fig. 2 shows the flowchart of the proposed FVC estimation method. The coarse resolution GLASS FVC data from MODIS are used to constrain the dynamic vegetation growth models with temporal dependencies for each Landsat 7 ETM+ pixel. Then, the radiative transfer model is used to establish the relationship between spectral reflectance and FVC. Finally, FVC is modeled at the finer-scale Landsat resolution based on the above two components in a DBN probabilistic framework.

A. Dynamic Vegetation Growth Model

Many dynamic vegetation growth models including mechanical, semimechanical and statistical models have been developed to characterize the vegetation growth characteristics [15], [16]. Compared to the mechanical or semi-mechanical models, the statistical dynamic vegetation growth model usually has simpler mathematical representation and less input parameters. Therefore, a statistical dynamic vegetation growth model is selected in this letter. The GLASS FVC data, which could represent vegetation growth and dynamics under climatic conditions and phenology, are temporally rich with high data quality. Thus, time series GLASS FVC data are employed to construct the dynamic vegetation growth model and build temporal dependencies.

1) Time-Efficient Dynamic Vegetation Growth Model: A time-efficient dynamic vegetation growth model incorporated in the FVC estimation process to describe vegetation growth for each ETM+ pixel is constructed as follows:

$$\mathrm{FVC}_t = P_t \times \mathrm{FVC}_{t-1} \tag{1}$$

where FVC_t represents FVC at current time, FVC_{t-1} is FVC at the previous time. P_t is the operator term and calculated by

$$P_t = 1 + \frac{\Delta T}{k(t) + \varepsilon} \times \frac{dk(t)}{dt} \tag{2}$$

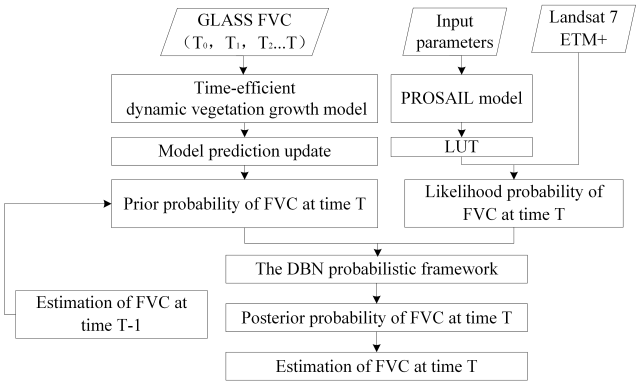

Fig. 2. Flowchart of the proposed method based on the radiative transfer model and the vegetation dynamic model.

where $\triangle T$ is the time step and $k(t)$ is the preprocessed and resampled GLASS FVC at time T using a decomposition method [9]. It is used as trend line to constrain the dynamic vegetation growth model. ε is set to 10^{-3} to prevent a null denominator. $(dk(t)/dt)$ is calculated from GLASS FVC at time t and $t-1$. In (1), the model assumes that FVC at current state is transitioned from previous FVC state and the change extent could be determined by the operator term P_t. The model takes advantage of the variation tendency of GLASS FVC dynamics, which is assumed to agree with the realities of ground vegetation growth. Observed FVC data covering the whole vegetation growth cycle is not required to build this dynamic vegetation growth model. The state transition process represented by the dynamic vegetation growth model is embedded in the DBN FVC estimation framework. When new observations are joined, they could be used for FVC estimation at the updated moment.

2) Modified Verhulst Logistic Equation: To compare the time efficiency among the dynamic vegetation growth models, the modified Verhulst logistic equation is also employed to combine with the radiative transfer model for FVC estimation. The generalized form of the modified Verhulst logistic equation is shown as follows:

$$\mathrm{FVC} = \frac{d}{1 + \exp(a \times t^2 + b \times t + c)} \tag{3}$$

where t is DOY, the independent variables, a, b, c, and d are model parameters. The Universal Global Optimization (UGO) algorithm was used to determine the initial guess and the Levenberg–Marquardt (LM) algorithm was selected to solve the curve-fitting problem to fit the four coefficients. The iterative procedure stops when the minimum of the sum of the squares is achieved. The fitting process is a very time consuming iterative procedure.

B. PROSAIL Model and LUT

The PROSPECT model coupled with SAIL model (PROSAIL) model [17] was selected to establish the relationship between the reflectance of remote sensing data and FVC in this letter. Equation (4) describes how the simulated canopy reflectance is generated from the simulation of PROSAIL model

$$\rho = \mathrm{PROSAIL}(\mathrm{LAI}, \mathrm{ALA}, N, C_{\mathrm{ab}}, C_m, C_{\mathrm{ar}}, C_w, C_{\mathrm{brown}}, \mathrm{Hot}, \mathrm{SZA}, \mathrm{VZA}, \mathrm{RAZ}, \rho_s) \tag{4}$$

where N is leaf structure parameter, C_{ab} is leaf chlorophyll a + b concentration, C_m is dry matter content, C_w is water content, C_{ar} is carotenoid content, C_{brown} is brown pigment content [17], LAI is leaf area index, ALA is average leaf angle inclination, Hot is hot-spot parameter, and ρ_s is soil reflectance. LAI was converted from FVC (Table I) using the following [18]:

$$\mathrm{Po}(\theta) = \exp\left(-\frac{G(\theta, \mathrm{LIDF})}{\cos(\theta)}\right) \times \mathrm{LAI} \tag{5}$$

$$\mathrm{FVC} = 1 - \mathrm{Po}(0^\circ) \tag{6}$$

where Po(θ) and G(θ, LIDF) is the gap fraction ($\theta = 0^\circ$ for nadir view) and projection function, respectively. LIDF is the leaf inclination distribution function. The input parameters of PROSAIL were set mainly based on the Leaf Optical Properties Experiment 93 (LOPEX'93) database. Then the LUTs, totally including 123 750 combinations of FVC and the corresponding simulated reflectance, are generated. The 2-D conditional probability distributions (CPDs), which describe the frequency distribution of red and near-infrared response (NIR) reflectance captured by Landsat ETM+ sensor corresponding to a certain FVC value (in its step of range shown in Table I), are calculated through a statistical analysis of LUTs and saved in conditional probability tables (CPTs).

TABLE I
INPUT PARAMETERS IN THE PROSAIL MODEL

Model	Parameter	Units	Range (or Value)	Step
PROSPECT	C_{ab}	$\mu g/cm^2$	20-60	10
	C_m	g/cm^2	0.01	-
	C_{ar}	$\mu g/cm^2$	0	-
	C_w	cm	0.02	-
	C_{brown}	-	0	-
	C_{ant}	$\mu g/cm^2$	0	-
	N	-	1.5	-
SAIL	FVC	-	0.01-0.99	0.01
	ALA	∘	15-60	5
	SZA	∘	25-45	5
	Hot	-	0.25	-

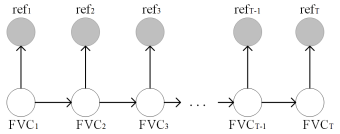

Fig. 3. Diagram of DBN in time series.

C. DBN Probabilistic Framework

Fig. 3 shows a diagram of the DBN probabilistic framework in this letter. The arcs connecting the FVC nodes (FVC_1, FVC_2, ... , FVC_{T-1}, FVC_T) represent state transition relationship in the time series and the arcs pointing from FVC nodes to Ref nodes (Ref_1, Ref_2, ... , Ref_{T-1}, Ref_T) donate the dependence relationship. This DBN used for FVC estimation integrates the remote sensing data, dynamic vegetation growth model, and radiative transfer model to obtain optimal FVC estimation. Equation (7) shows the basic structure of the DBN for FVC estimation [8], [9]

where Ref_T donates the Landsat 7 ETM+ reflectance data at time T, FVC_T represents the true value of FVC at time T. $\mathrm{P}(\mathrm{FVC}_T|\mathrm{Ref}_T)$ is the posterior probability distribution of FVC at time T, $\mathrm{P}(\mathrm{FVC}_{T-1}|\mathrm{Ref}_{T-1})$ is the posterior probability distribution of FVC at time $T-1$. $\mathrm{P}(\mathrm{ref}_T|\mathrm{FVC}_T)$ is the likelihood probability from remote sensing observations combining LUTs and CPTs generated from PROSAIL model. $\mathrm{P}(\mathrm{FVC}_T|\mathrm{FVC}_{T-1})$ is the state transition probability from the dynamic vegetation growth model. Denominator of the part

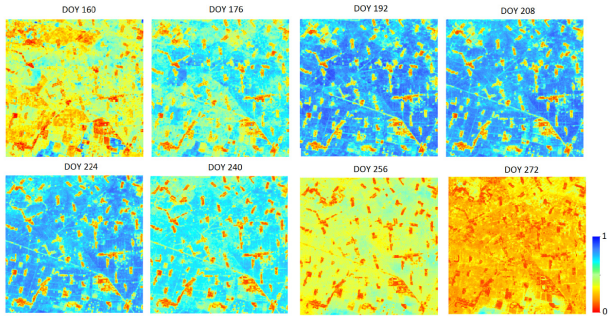

Fig. 4. FVC maps from DOY 160 to DOY 272 in the year 2012 generated using the proposed method.

to the right of the equal sign is the normalization term. Equation (7) is calculated as the following steps. First, the vegetation dynamic growth model predicted FVC of each Landsat 7 ETM+ pixel at time T is updated (Section III-A). Then, $\mathrm{P}(\mathrm{FVC}_T|\mathrm{FVC}_{T-1})$ is calculated using the normal cumulative function (where μ is set to model predicted FVC and σ is set to model error). Next, $\mathrm{P}(\mathrm{ref}_T|\mathrm{FVC}_T)$ is determined by probability of Landsat 7 ETM+ reflectance located in discrete intervals (which is obtained assuming Landsat 7 ETM+ reflectance obeys Gaussian distribution) multiplying by CPDs. Finally, the posterior probability distribution $\mathrm{P}(\mathrm{ref}_T|\mathrm{FVC}_T)$ is calculated and then the optimal FVC value is estimated from $\mathrm{P}(\mathrm{ref}_T|\mathrm{FVC}_T)$ using the minimum mean square error (MMSE) estimation method.

IV. Results

FVC maps from DOY 160 to DOY 272 in the year 2012 derived from Landsat 7 ETM+ data and GLASS FVC product using the proposed method are shown in Fig. 4. Before DOY 160 or after DOY 272, vegetation is sparse in the study area because the meteorological conditions are not suitable for plant growth during these periods. Therefore, relatively complete vegetation growing season of the study area (generally from late-April to late-August) was covered in the maps. The spatial distribution and temporal FVC changes were consistent with the actual land cover types in these maps. After a rapid growing period since DOY 160, the FVC values reached a maximum at around DOY 192–208. Then, the FVC values gradually decreased until around DOY 272, which indicated the planted crops reached its mature state.

Fig. 5 shows the scatter plots of the estimated FVC from the estimating process incorporating different kinds of dynamic vegetation growth models (the time-efficient model proposed in this letter and the modified Verhulst logistic equation) and ground measured FVC. The FVC estimation accuracy using a time-efficient dynamic vegetation growth model is satisfactory ($R^2 = 0.889$, RMSE $= 0.0917$) and comparable to that from the previously developed inefficient but well-established method incorporating the dynamic vegetation growth model represented by the modified Verhulst logistic equation [8] ($R^2 = 0.884$, RMSE $= 0.0913$).

To access the degree of conformity between the FVC estimates and vegetation growth characteristics, temporal trajectories of the estimated FVC in this letter, GLASS FVC and

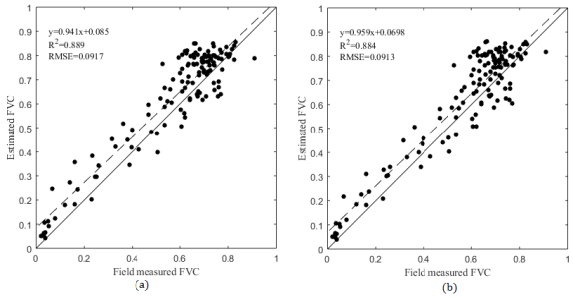

Fig. 5. Validation of the FVC estimation method incorporating (a) Time efficient dynamic vegetation growth model proposed in this letter. (b) Modified Verhulst logistic equation.

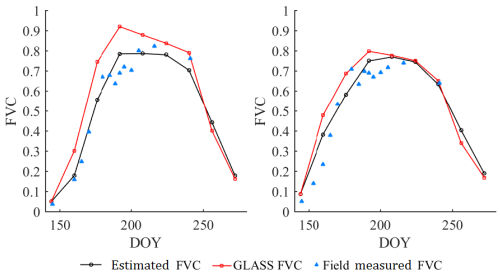

Fig. 6. Comparison between estimated FVC in this letter, GLASS FVC and field measured FVC in time series.

TABLE II
Model Computational Costs

Dynamic vegetation growth model	Time used for fitting parameters	Time used for DBN	Total time
The proposed method	-	86.55s	86.55s
The modified Verhulst logistic equation	77533.67s	84.91s	77618.58s

field measured FVC at two randomly selected sample sites in the year 2012 are shown in Fig. 6. It is obvious that the estimated FVC using the proposed method fell closer to the field measured FVC. Most of the field measured data distributes around the temporal trajectories of the estimated FVC. The estimated FVC was consistent with actual vegetation cover change and tend to reflect better of the rapid growing stage of crops in the study area.

Table II shows the average computational cost of FVC estimation method incorporating the time-efficient dynamic vegetation growth model. This comparison experiment is conducted using images with size of 200 × 200 pixels. All calculations are carried out using the Matlab software (The Mathwork, Inc., Natick, MA, USA) on a single PC installed with a Windows 7 64-bit operating system, with Intel i7-4790 CPU, 12 GB of main memory. Each process is conducted ten times and the average elapsed time is calculated. To compare time cost, the modified Verhulst logistic equation is substituted for the dynamic vegetation growth model in the FVC estimation method and its average computational cost is also shown in Table II. Much more time is spent on fitting model parameters of the modified Verhulst logistic equation. Relatively, the time-efficient dynamic vegetation

$$P(\mathrm{FVC}_T|\mathrm{Ref}_T) = \frac{P(\mathrm{ref}_T|\mathrm{FVC}_T)\sum_{\mathrm{FVC}_{T-1}} P(\mathrm{FVC}_T|\mathrm{FVC}_{T-1})P(\mathrm{FVC}_{T-1}|\mathrm{Ref}_{T-1})}{\sum_{\mathrm{FVC}_T} P(\mathrm{ref}_T|\mathrm{FVC}_T)P(\mathrm{FVC}_T|\mathrm{Ref}_{T-1})} \tag{7}$$

growth model proposed in this letter saved time for parameter fitting. Therefore, it is much faster and suitable for application of the proposed method on larger scales. It has great potential to be applied for real-time FVC estimation on large scale.

V. Discussion

This letter proposed a Landsat scale FVC estimation method incorporating dynamic vegetation growth information which is time-efficient and suitable for near real-time FVC estimation. Most of the commonly used FVC estimation methods, such as empirical methods [19], pixel unmixing methods [20], and machine learning methods [3], only take advantage of remote sensing data at a single time slice. Compared to these methods, the proposed method utilizes multitemporal remote sensing observations to constrain the model with temporal dependencies and weaken influences caused by atmosphere and aerosol.

Besides, the dynamic vegetation growth model constructed in this letter is computationally efficient compared to the commonly used statistical dynamic vegetation growth models, such as the Richards plant growth model [21], and logistic growth models [22], which often need iterative or regression process to fit model parameters and cost much computing time. Compared to mechanical or semimechanical dynamic vegetation growth models which are often complicated and require a series of model driving parameters, the proposed dynamic vegetation growth model is much easier to implement. The computational time has a linear relationship to the number of pixels because the dynamic vegetation growth model is built for each pixel without utilizing the information of other pixels. The proposed method is also suitable for real-time FVC estimation because it does not require FVC observations covering the whole vegetation growth cycle to build the dynamic vegetation growth model. New observations could be added to the FVC estimation process of the proposed method as soon as they are available. Therefore, the proposed method has the potential to provide high quality and high spatial resolution FVC product at large scales. However, this letter also has some limitations. Only 13 sample sites were available and the relatively low number of samples may potentially lead to low representative level of vegetation and random error. In addition, the study area is mainly covered with planted maize and the surface around the sample site is deemed homogeneous and spatially continuous. Therefore, FVC of the 10 m $\times$ 10 m sample is considered to be the same with the corresponding 30 m resolution pixel and used for validation. In further study, more samples with the same size of Landsat pixels should be collected for validation to avoid potential problems brought by low number and small samples.

VI. Conclusion

This letter proposed a method which improves the capability of FVC estimation at Landsat scale based on coarse spatial resolution (500 m) GLASS FVC data. The method facilitated development of a time-efficient dynamic vegetation growth model and radiative transfer models linking Landsat 7 ETM+ reflectance to FVC, and all combined in a probabilistic DBN framework. The proposed method has high computational efficiency and is feasible for real-time FVC estimation. The method could also be applied to other similar or higher spatial resolution data such as CBERS, GF-1 and Sentinael-2. Future work should focus on assessing the performance of the proposed method on generating reliable high spatial resolution FVC products at large scales.

References

[1] J.-L. Roujean and R. Lacaze, "Global mapping of vegetation parameters from POLDER multiangular measurements for studies of surface-atmosphere interactions: A pragmatic method and its validation," *J. Geophys. Res.*, vol. 107, no. D12, pp. 1–14, 2002.

[2] G. Gutman and A. Ignatov, "The derivation of the green vegetation fraction from NOAA/AVHRR data for use in numerical weather prediction models," *Int. J. Remote Sens.*, vol. 19, no. 8, pp. 1533–1543, 1998.

[3] K. Jia *et al.*, "Fractional vegetation cover estimation algorithm for Chinese GF-1 wide field view data," *Remote Sens. Environ.*, vol. 177, pp. 184–191, May 2016.

[4] A. A. Gitelson, Y. J. Kaufman, R. Stark, and D. Rundquist, "Novel algorithms for remote estimation of vegetation fraction," *Remote Sens. Environ.*, vol. 80, no. 1, pp. 76–87, Jun. 2001.

[5] L. Yang, K. Jia, S. Liang, X. Wei, Y. Yao, and X. Zhang, "A robust algorithm for estimating surface fractional vegetation cover from landsat data," *Remote Sens.*, vol. 9, no. 8, p. 857, 2017.

[6] P. D. Jamieson, M. A. Semenov, I. R. Brooking, and G. S. Francis, "*Sirius*: A mechanistic model of wheat response to environmental variation," *Eur. J. Agronomy*, vol. 8, nos. 3–4, pp. 161–179, 1998.

[7] X. Wang, K. Jia, S. Liang, and Y. Zhang, "Fractional vegetation cover estimation method through dynamic Bayesian network combining radiative transfer model and crop growth model," *IEEE Trans. Geosci. Remote Sens.*, vol. 54, no. 12, pp. 7442–7450, Dec. 2016.

[8] X. Wang *et al.*, "Estimating fractional vegetation cover from landsat-7 ETM+ reflectance data based on a coupled radiative transfer and crop growth model," *IEEE Trans. Geosci. Remote Sens.*, vol. 55, no. 10, pp. 5539–5546, Oct. 2017.

[9] Y. Tu, K. Jia, S. Liang, X. Wei, Y. Yao, and X. Zhang, "Fractional vegetation cover estimation in heterogeneous areas by combining a radiative transfer model and a dynamic vegetation model," *Int. J. Digit. Earth*, to be published.

[10] W. Song, X. Mu, G. Yan, and S. Huang, "Extracting the green fractional vegetation cover from digital images using a shadow-resistant algorithm (SHAR-LABFVC)," *Remote Sens.*, vol. 7, no. 8, pp. 10425–10443, Aug. 2015.

[11] K. Jia *et al.*, "Global land surface fractional vegetation cover estimation using general regression neural networks from MODIS surface reflectance," *IEEE Trans. Geosci. Remote Sens.*, vol. 53, no. 9, pp. 4787–4796, Sep. 2015.

[12] K. Jia *et al.*, "Validation of global LAnd surface satellite (GLASS) fractional vegetation cover product from MODIS data in an agricultural region," *Remote Sens. Lett.*, vol. 9, no. 9, pp. 847–856, 2018.

[13] J. Chen, P. Jönsson, M. Tamura, Z. Gu, B. Matsushita, and L. Eklundh, "A simple method for reconstructing a high-quality NDVI time-series data set based on the Savitzky–Golay filter," *Remote Sens. Environ.*, vol. 91, nos. 3–4, pp. 332–344, 2004.

[14] X. Zhu, D. Liu, and J. Chen, "A new geostatistical approach for filling gaps in Landsat ETM+ SLC-off images," *Remote Sens. Environ.*, vol. 124, pp. 49–60, Sep. 2012.

[15] J. Eitzinger, M. Trnka, J. Hösch, Z. Žalud, and M. Dubrovský, "Comparison of CERES, WOFOST and SWAP models in simulating soil water content during growing season under different soil conditions," *Ecol. Model.*, vol. 171, no. 3, pp. 223–246, 2004.

[16] J. W. Jones *et al.*, "The DSSAT cropping system model," *Eur. J. Agronomy*, vol. 18, nos. 3–4, pp. 235–265, 2003.

[17] S. Jacquemoud *et al.*, "PROSPECT + SAIL models: A review of use for vegetation characterization," *Remote Sens. Environ.*, vol. 113, pp. S56–S66, Sep. 2009.

[18] G. S. Campbell, "Extinction coefficients for radiation in plant canopies calculated using an ellipsoidal inclination angle distribution," *Agricult. Forest Meteorol.*, vol. 36, no. 4, pp. 317–321, 1986.

[19] J. Xiao and A. Moody, "A comparison of methods for estimating fractional green vegetation cover within a desert-to-upland transition zone in central New Mexico, USA," *Remote Sens. Environ.*, vol. 98, nos. 2–3, pp. 237–250, 2005.

[20] J. C. Jiménez-Muñoz, J. A. Sobrino, A. Plaza, L. Guanter, J. Moreno, and P. Martinez, "Comparison between fractional vegetation cover retrievals from vegetation indices and spectral mixture analysis: Case study of PROBA/CHRIS data over an agricultural area," *Sensors*, vol. 9, no. 2, pp. 768–793, 2009.

[21] A. Gregorczyk, "Richards plant growth model," *J. Agronomy Crop Sci.*, vol. 181, no. 4, pp. 243–247, 1998.

[22] A. Tsoularis and J. Wallace, "Analysis of logistic growth models," *Math. Biosci.*, vol. 179, no. 1, pp. 21–55, 2002.